Irreversibility of a quantum walk induced by controllable decoherence employing random unitary operations*

Xu You-Yang(徐酉阳)[a], Zhou Fei(周 飞)[b], Chen Liang(陈 亮)[b], Xie Yi(谢 艺)[b,c], Xue Peng(薛 鹏)[d], and Feng Mang(冯 芒)[b,†]

[a] *Faculty of Science, Kunming University of Science and Technology, Kunming* 650093, *China*

[b] *State Key Laboratory of Magnetic Resonance and Atomic and Molecular Physics, Wuhan Institute of Physics and Mathematics, Chinese Academy of Sciences, Wuhan* 430071, *China*

[c] *Graduate School of the Chinese Academy of Sciences, Beijing* 100049, *China*

[d] *Department of Physics, Southeast University, Nanjing* 211189, *China*

(Received 24 September 2011; revised manuscript received 29 November 2011)

Quantum walk is different from random walk in reversibility and interference. Observation of the reduced reversibility in a realistic quantum walk is of scientific interest in understanding the unique quantum behavior. We propose an idea to experimentally investigate the decoherence-induced irreversibility of quantum walks with trapped ions in phase space via the average fidelity decay. By introducing two controllable decoherence sources, i.e., the phase damping channel (i.e., dephasing) and the high temperature amplitude reservoir (i.e., dissipation), in the intervals between the steps of quantum walk, we find that the high temperature amplitude reservoir shows more detrimental effects than the phase damping channel on quantum walks. Our study also shows that the average fidelity decay works better than the position variance for characterizing the transition from quantum walks to random walk. Experimental feasibility to monitor the irreversibility is justified using currently available techniques.

Keywords: quantum walk, irreversibility, trapped ions, average fidelity decay

PACS: 03.65.Yz, 42.50.Ex, 05.40.Fb **DOI:** 10.1088/1674-1056/21/4/040304

1. Introduction

The random walk is an important concept widely applied in different scientific fields including astronomy, solid-state physics, polymer chemistry, biology, and even the stock market. In particular, many powerful classical algorithms, e.g., graph connectivity[1] and k-th satisfiability problems,[2] are based on random walks. The quantum walk (QW) is a quantum mechanical counterpart of the random walk, which outperforms random walk in some computational tasks, such as the black box problem,[3,4] the search in an unstructured database,[5] and quantum simulations of classical annealing processes.[6] It has also been found that the QW can work as a universal computational primitive.[7]

The QW has been experimentally realized with optically confined atoms,[8] trapped ions,[9,10] and photons.[11,12] It has been shown that the spatial distribution is very different between the QW and the random walk, in which the QW spreads linearly in time while the random walk spreads as the square root of time. However, under the influence of some kinds of noisy environments,[13−22] a QW might be finally degenerated to a random walk with decoherence increasing. Via the spatial distribution, the difference between the QW and random walk was studied experimentally with trapped ions in phase space through controllable decoherence on the coin,[10] and the transition from the QW to random walk has been demonstrated with individual photons in space by changing the types of decoherence applied to the system.[12] However, one of the typical characteristics of the QW reducing to the random walk is the irreversibility due to the increasing classicality, and it is of great interest to show the variation of the irreversibility in the time evolution of the QW. Some approaches, such as the mean phonon number[23] and the linear entropy,[24] to study the irreversibility have been developed recently. However those approaches are not operational, that means neither of them provides a way for direct experimental observation of the irreversibility of the

*Project supported by the National Natural Science Foundation of China (Grant Nos. 10974225, 10944005, and 11004029).

†Corresponding author. E-mail: mangfeng@wipm.ac.cn

© 2012 Chinese Physical Society and IOP Publishing Ltd

QW, and we will propose a quantity, called the average fidelity decay (AFD), to measure this irreversibility, which can be observed experimentally. We also note that not all of the decoherence can degenerate the QW to random walk,[25] and the reason is not yet clear. Nevertheless, decoherence will surely induces the irreversibility.

In this work, we propose an idea using trapped ions for experimentally observing the irreversibility of the QW due to decoherence. Two kinds of decoherence sources, i.e., the phase damping channel or called dephasing, and the high temperature amplitude reservoir, which is a dissipative source, are controllably introduced into the trapped-ion system. To clarify the decoherence effect on the QW, we only consider below the ideal QW influenced by the man-made decoherence, i.e., with the decoherence inserted into the intervals between the steps of the QW. This is modeled based on the fact that the QW experiments with trapped ions could be accomplished nearly ideally.[9,10] The controllable decoherence is introduced by random unitary operations U_{ζ_m} alternately applied after each steps of the QW, where the perturbation parameter ζ_m is a random variable for the m-th perturbation. As the perturbation is introduced repeatedly, we have $U_{\Delta} = \prod_{m=1}^{N}(U_{\zeta_m}U_{\rm QW})$, with the subscript Δ representing the perturbation, and the decoherence can be introduced through the ensemble average, i.e., $\langle U_{\Delta}|\phi_0\rangle\langle\phi_0|U_{\Delta}^{\dagger}\rangle_{\Delta}$ with the angle bracket representing an average over the perturbation Δ. It has been shown that $\langle U_{\Delta}|\phi_0\rangle\langle\phi_0|U_{\Delta}^{\dagger}\rangle_{\Delta}$ satisfies the master equation subject to the perturbation-relevant decoherence.[26]

This article is arranged as follows. The decoherence sources are introduced into the QW in the next section, and we explore the feasibility to observe the irreversibility by monitoring the changes of the AFD in Section 3. A brief summary is given in the last section.

2. QW with two ions under decoherence

Each single step of QW contains two sub-steps, i.e., the coin toss and the coin state-dependent displacement, corresponding to the unitary operation below,

$$U_{\rm QW} = {\rm e}^{-{\rm i}\,\alpha\hat{p}\hat{\sigma}_2^z}\tilde{H}_2, \tag{1}$$

where $\hat{p} = {\rm i}\sqrt{\hbar M\omega_l}(\hat{a}^{\dagger} - \hat{a})/\sqrt{2}$ is the momentum operator with M the mass of the ion, $\hat{a}$ (ω_l) is the annihilation operator (frequency) of the axial center-of-mass mode, and α is the step size of the QW. $\hat{\sigma}_2^z$ is the Pauli operator on the coin, and

$$\tilde{H}_2 = \frac{\begin{pmatrix} 1 & 1 \\ 1 & -1 \end{pmatrix}}{\sqrt{2}}$$

is the Hadamard gate on the internal states of the second ion for the coin toss. According to Refs. [9] and [10], the state-dependent displacement operator is implemented by applying a state-dependent force on the ion and the coin toss operator H is applied on the ion by two "carrier" transitions.

We make use of two trapped ions to simulate the QW under decoherence, where the coin is represented by the internal states of the second trapped ion, and the positions of the walker are encoded into the coherent states of the axial center-of-mass mode of both the ions. Decoherence is introduced in between each QW steps, which follows the idea in Ref. [10] and could reduce the complexity and challenge in experimental implementation. This is also helpful for understanding the impact due to decoherence in a clear and simpler physical picture. The first ion is employed for two purposes: the decoherence-induced perturbation is applied on the first ion which is then reflected to the second ion via the motional states and the measurement is made on the first ion. The decoherence of the coin is due to the phase damping channel, and the high temperature amplitude reservoir acts on the walker's position, where the high temperature amplitude reservoir is applied to the axial center-of-mass mode directly, but the phase damping channel is introduced via the transverse modes to avoid interrupting the walker's position.

The key point of our scheme is that the presence (absence) of the decoherence resulting in the QW behavior corresponds to the population in the lower (upper) internal state of the first ion. As a result, provided a superposition of the internal states of the first ion, the second ion would evolve under different conditions simultaneously. We will show the experimental feasibility to measure the AFD from the level occupation of the first ion, which implies a possibility to monitor the QW reducing to the random walk under decoherence. The AFD is defined based on fidelity decay, that is the square modulus of the overlap between two time-dependent final states with the same initial state $|\phi_0\rangle$ but respectively, under the unperturbed evolution U and perturbed evolution U_{Δ}. Different from the fidelity, the fidelity decay focuses on

the overlap of the initial state with the final state under an unperturbed evolution U and then a perturbed echo U_Δ. After averaging over the perturbation, the AFD is defined as[27]

$$\bar{F} = \langle |\langle \phi_0 | U_\Delta^\dagger U | \phi_0 \rangle|^2 \rangle_\Delta. \quad (2)$$

The AFD can reveal the response of the system to the environmental perturbation, which is closely related to the properties of both the system and the environmental perturbation.

To demonstrate the irreversibility more clearly, we will compare the AFD with the position variance which is defined as

$$\delta = \langle \langle \phi_0 | U_\Delta^\dagger (\hat{x} - \bar{x})^2 U_\Delta | \phi_0 \rangle \rangle_\Delta, \quad (3)$$

with $\hat{x} = \sqrt{\hbar}(\hat{a} + \hat{a}^\dagger)/\sqrt{2M\omega_l}$ being the position operator and $\bar{x}$ the average of the position. As the position variance usually shows similar behaviors under different decoherence sources,[17−20] we study the change of the AFD under the two decoherence sources with the same parameters as in calculating the position variance, which helps us to understand the irreversibility in the QW.

2.1. QW under the phase damping channel

The first decoherence source we consider is the phase damping channel, i.e., dephasing on the coin.[28] To avoid interrupting the walker's position encoded in the axial mode, we design the coupling of the two ions via the radial modes, as shown in Fig. 1(a). By eliminating the excited state adiabatically and under the rotating wave approximation, we have the interaction Hamiltonian as[29]

$$H_1 = \sum_{\substack{s=+,-\\ i=1,2}} \{\chi_{i,s} + [\Omega_{i,s}\, \mathrm{e}^{\mathrm{i}\,\eta_r(\hat{b}+\hat{b}^\dagger) - \mathrm{i}(\omega_r+\delta)t} + \mathrm{H.c.}]\} \otimes |s\rangle_i\langle s|, \quad (4)$$

where $\chi_{i,s}$ and $\Omega_{i,s}$ are, respectively, the time-averaged Stark shift and AC Stark shift of the i-th ion's state $|s\rangle_i$. $\hat{b}$ (ω_r) is the annihilation operator (frequency) of the radial center-of-mass mode, δ is the detuning of the laser frequency difference from the radial center-of-mass mode frequency, and η_r is the corresponding Lamb–Dicke parameter. By choosing appropriate polarization of the lasers, we may have the AC Stark shifts to be $\Omega_{1,-} = 0$, $\Omega_{1,+} = \Omega_1$, and $\Omega_{2,+} = -\Omega_{2,-} = \Omega_2$, which reduce Eq. (4) to

$$H_2 = \sum_{i=1,2} \hat{A}_i [\Omega_i\, \mathrm{e}^{\mathrm{i}\,\eta_r(\hat{b}+\hat{b}^\dagger) - \mathrm{i}(\omega_r+\delta)t} + \mathrm{H.c.}], \quad (5)$$

where $\hat{A}_1 = |+\rangle_1\langle +|$, $\hat{A}_2 = \hat{\sigma}_2^z$, and the zero AC Stark shift could be achieved by setting the direction of the laser polarization to be orthogonal to the corresponding electric dipole of the ion. We have neglected the time-averaged Stark shifts in Eq. (5) due to proper single-qubit operations. In a rotating frame with respect to the radial frequency ω_r, the above Hamiltonian could be further simplified under Lamb–Dicke limit and rotating wave approximation,

$$H_3 = \eta_r(\Omega_1 |+\rangle_1\langle +| + \Omega_2 \hat{\sigma}_2^z)(\hat{b}\, \mathrm{e}^{-\mathrm{i}\,\delta t} + \hat{b}^\dagger\, \mathrm{e}^{\mathrm{i}\,\delta t}). \quad (6)$$

The corresponding operation is given by[30,31]

$$U_1 = \exp\{\mathrm{i}[(\phi_1 |+\rangle_1\langle +| + \phi_2 \hat{\sigma}_2^z)\hat{b} + \mathrm{H.c.}] + \mathrm{i}\,\kappa |+\rangle_1\langle +| \otimes \hat{\sigma}_2^z\}, \quad (7)$$

where $\phi_i(T) = \Omega_i \int_0^T \mathrm{e}^{\mathrm{i}\,\delta t}\mathrm{d}t$ with i =1, 2 and $\kappa(T) = 2\eta_r^2 \Omega_1 \Omega_2 \int_0^T \mathrm{d}t_2 \int_0^{t_2} \sin\delta(t_2 - t_1)\mathrm{d}t_1$. Under the condition $\delta T = 2k\pi$, with k an integer, we have $\phi_i(T) = 0$ and $\kappa(T) = 4k\pi[\eta_r^2 \Omega_1 \Omega_2/\delta^2]$, which reduce Eq. (7) to

$$U_2 = \mathrm{e}^{\mathrm{i}\,\kappa |+\rangle_1\langle +| \otimes \hat{\sigma}_2^z}. \quad (8)$$

So κ is actually the perturbation applied on the second ion via the first ion. We may denote κ by ζ_m^c meaning the m-th perturbation on the coin. By randomly choosing Ω_i, we have this phase to be a random number from a uniform distribution $\zeta^c \in (-q\pi, q\pi)$, where $q = 0$ corresponds to the QW and $q = 1$ to the random walk. Our study in the general case will be on $0 < q < 1$. Equation (8) implies the perturbation, with the evolution operator

$$U_{\Delta_c} = \prod_{m=1}^{n} (U_{\zeta_m^c} U_{\mathrm{QW}}), \quad (9)$$

where $U_{\zeta_m^c} = \exp[\mathrm{i}\,\zeta_m^c \hat{\sigma}_2^z]$ is applied on the second ion only in the case of the first ion in $|+\rangle_1$. For the first ion in $|-\rangle_1$, the time evolution of the QW is under the unperturbed evolution operator $U = U_{\mathrm{QW}}^n$.

2.2. QW under the high temperature amplitude reservoir

The second controllable decoherence source is the high temperature amplitude reservoir, i.e., the dissipation, on the walker's position. The high temperature amplitude reservoir has been applied on the cat states of the trapped ions,[32,33] presenting the decoherence rate scaling with the size of the superposition state. In our case, we apply a state-dependent force on the first

ion, as shown in Fig. 1(b), which couples the internal state $|+\rangle_1$ to the corresponding axial center-of-mass mode. Using the similar treatment to the phase damping channel case, we choose $\Omega_{1,-} = \Omega_{2,+} = \Omega_{2,-} = 0$, $\Omega_{1,+} = \Omega$, and the laser frequency difference equal to the axial center-of-mass mode frequency ω_l, which yields the interaction Hamiltonian,

$$H_4 = \eta_l \Omega \hat{x} \otimes |+\rangle_1\langle +|, \tag{10}$$

where η_l is the corresponding Lamb–Dicke parameters. As for the phase damping channel, if the first ion is prepared in state $|-\rangle_1$, there is no perturbation on the walker's position, and the perturbation works only if the first ion is prepared in state $|+\rangle_1$, with the corresponding evolution operator

$$U_{\Delta_p} = \prod_{m=1}^{n} (U_{\zeta_m^p} U_{\mathrm{QW}}), \tag{11}$$

where $U_{\zeta_m^p} = \mathrm{e}^{-\mathrm{i}\,\zeta_m^p \hat{x}}$ is the m-th perturbation on the position of the walker and $\zeta_m^p = \eta_l \Omega_m \tau$ with τ the pulse length of the perturbation. Similar to the above variable ζ_m^c, the variable ζ_m^p is chosen as a random number changing in a uniform distribution $\zeta^p \in (-q'\pi, q'\pi)$ with $0 < q' < 1$.

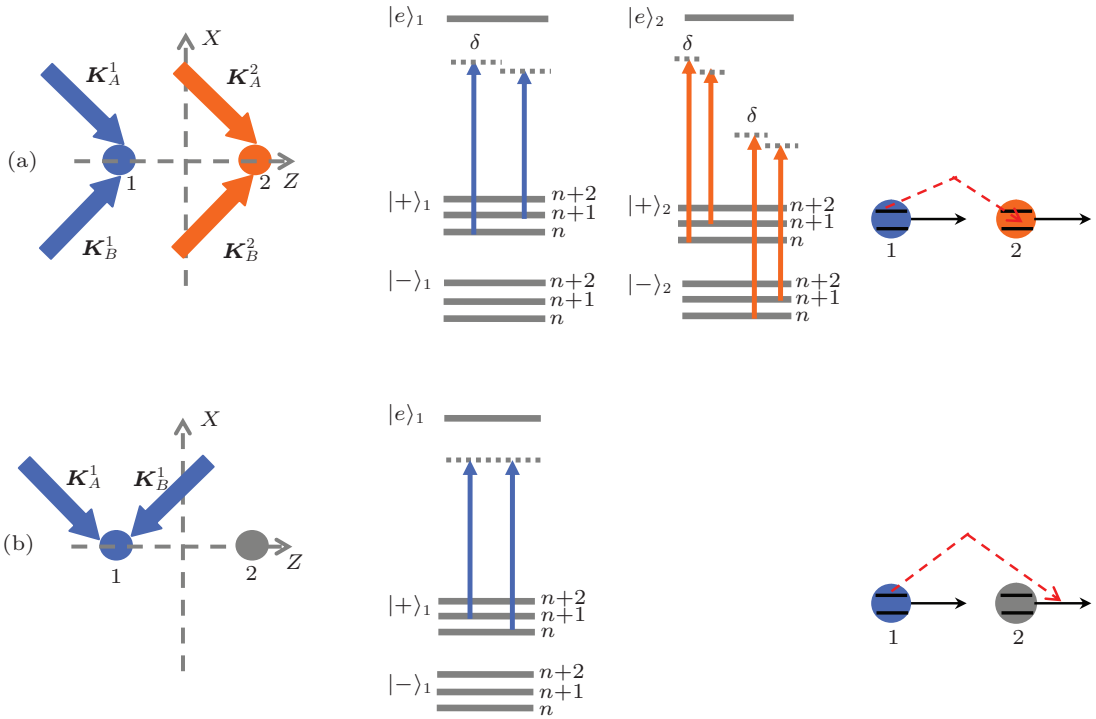


Fig. 1. (colour online) (a) The laser scheme to produce the state-dependent perturbation on the coin. Two pairs of lasers illuminate two ions individually, one pair of which on the first ion virtually excites the state $|e\rangle_1$ from $|+\rangle_1$ only, and another pair virtually excites the state $|e\rangle_2$ from both $|+\rangle_2$ and $|-\rangle_2$. Both the frequency differences are set to be $\omega_r + \gamma$, with $\gamma \ll \omega_r$, and both the wavevector differences, $\boldsymbol{K}_A^1 - \boldsymbol{K}_B^1$ and $\boldsymbol{K}_A^2 - \boldsymbol{K}_B^2$, are along the radial direction, which couple the radial mode to the internal state. The most right sketch shows that, the perturbation is equivalently introduced on the internal states of the second ion. (b) The laser scheme to produce the state-dependent perturbation on the walker's position, where the frequency difference between the lasers is set to be the same as the frequency ω_l and the wavevector difference of the lasers $\boldsymbol{K}_A^1 - \boldsymbol{K}_B^1$ is along the axial direction. The most right sketch shows that the perturbation is made on axial center-of-mass mode directly.

3. Discussion

3.1. Experimental observability

Experimental observation of the AFD is the key to study the QW with decoherence. For this purpose, we prepare the first ion in a superposition state $(|+\rangle_1 + |-\rangle_1)/\sqrt{2}$, and the coin and walker's position in state $|\phi_0\rangle_2$. Numerically we can produce N sequences of random numbers $\{\zeta_1, \ldots, \zeta_n\}_k$ $(k = 1, \ldots, N)$, chosen from a uniform distribution. After running n steps of the QW with perturbation parameters chosen above, the state becomes

$$\frac{1}{\sqrt{2}}(|+\rangle_1 U_\Delta |\phi_0\rangle_2 + |-\rangle_1 U |\phi_0\rangle_2). \tag{12}$$

Using a rotation operation R_x, transforming the state as $|+\rangle_1 \to (|+\rangle_1 + |-\rangle_1)/\sqrt{2}$ and $|-\rangle_1 \to (|+\rangle_1 - |-\rangle_1)/\sqrt{2}$, we can measure the populations in the state

$|+\rangle_1$ as,

$$P_k^x = \{1 + \mathrm{Re}\,[f_k]\}/2, \tag{13}$$

where $f_k = {}_2\langle\phi_0| U_{\Delta^k}^\dagger U |\phi_0\rangle_2$ is the amplitude of fidelity decay, with $U_{\Delta^k}^\dagger$ being $U_{\Delta_c^k}^\dagger$ or $U_{\Delta_p^k}^\dagger$ regarding the k-th sequence of the random numbers. Another rotation R_y making $|+\rangle_1 \to (|+\rangle_1 + \mathrm{i}\,|-\rangle_1)/\sqrt{2}$ and $|-\rangle_1 \to (|+\rangle_1 - \mathrm{i}\,|-\rangle_1)/\sqrt{2}$ leads to the measurement on the state $|+\rangle_1$ as

$$P_k^y = \{1 + \mathrm{Im}\,[f_k]\}/2. \tag{14}$$

We have to repeat the above steps by $N-1$ times to obtain a sequence of $\{f_k\}$, from which we can extract the AFD according to the following expression

$$\bar{F} = \frac{1}{N}\sum_k |f_k|^2. \tag{15}$$

From the relation $f_k = (2P_k^x - 1) + \mathrm{i}(2P_k^y - 1)$, observation of the AFD should be available by detecting the population of the internal levels of the ion.

3.2. Comparison between the phase damping channel and the high temperature amplitude reservoir

Using the AFD, we can know which decoherence source, phase damping channel or high temperature amplitude reservoir is more detrimental to the QW. As shown in Fig. 2, we have calculated both the AFD and position variance for the initial state $|\phi_0\rangle_2 = (|+\rangle_2 + |-\rangle_2)\,|0\rangle/\sqrt{2}$. Using the parameters which make position variance almost the same under the phase damping channel and high temperature amplitude reservoir, we find that the AFDs are different, particularly for big values of q. The AFDs under the high temperature amplitude reservoir are always smaller than those under the phase damping channel, implying the high temperature amplitude reservoir to be more detrimental than the phase damping channel to the QW. This result can be further understood by another definition of the AFD by Wigner function,[27]

$$\bar{F}' = \int W \cdot W_\Delta \,\mathrm{d}x\,\mathrm{d}p, \tag{16}$$

where W is the unperturbed Wigner function defined as[34]

$$W = \frac{1}{\pi^2}\int \mathrm{Tr}_p[\rho\, \mathrm{e}^{\eta(\hat{a}^\dagger - \beta)}\, \mathrm{e}^{\eta^*(\hat{a} - \beta^*)}]\, \mathrm{e}^{-1/2|\eta|^2}\, \mathrm{d}^2\eta \tag{17}$$

with $\beta = x + \mathrm{i}\,p$, and $\rho = \mathrm{Tr}_c[U\,|\phi_0\rangle_2\,\langle\phi_0|\,U^\dagger]$ the reduced density operator by tracing over the coin degrees of freedom. W_Δ is the perturbed Wigner function defined similarly to the unperturbed one, with ρ replaced by

$$\rho_\Delta = \mathrm{Tr}_c\left[\sum_{k=1}^{M} U_{\Delta_k}\,|\phi_0\rangle_2\,\langle\phi_0|\,U_{\Delta_k}^\dagger\right]\Big/M.$$

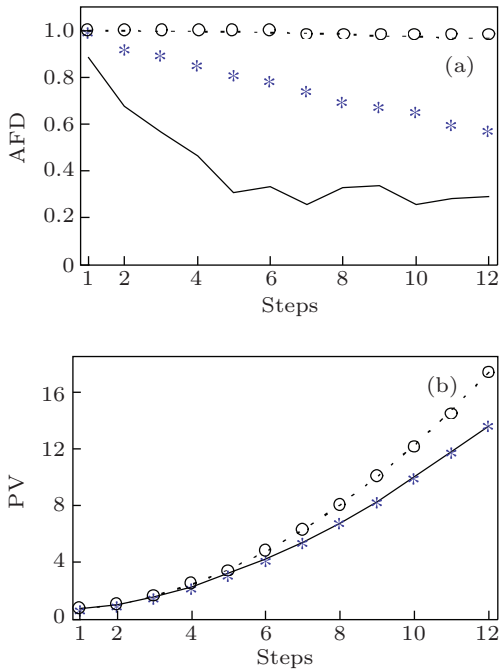


Fig. 2. (colour online) (a) AFDs under the phase damping channel and high temperature amplitude reservoir with the step size $\alpha = \sqrt{2}$, where the dotted and solid lines represent AFDs under the high temperature amplitude reservoir with the parameter $q' = 0.01$ and 0.18, respectively, and the circle and star correspond to the AFDs under the phase damping channel with $q = 0.02$ and 0.14, respectively. (b) The corresponding position variance under the same conditions in panel (a). With the values of q and q', the position variance for the phase damping channel and high temperature amplitude reservoir are almost the same in the short time period.

We have plotted the numerical results in Fig. 3, in which the unperturbed QW (Fig. 3(a)) corresponds to a Wigner function with negative values oscillating around the origin. The coherence of the QW is spoiled by the phase damping channel and high temperature amplitude reservoir, respectively, in Figs. 3(b) and 3(c), where the phase damping channel removes the nonclassical property (i.e., the negative values) of the Wigner function, whereas the high temperature amplitude reservoir broadens the fringes along the momentum. The introduction of the phase damping channel, as shown in Eq. (8), is actually related to the momentum operator (See Eq. (2)), which is equivalent to a random shift on the position displacement of the ion. In contrast, the high temperature amplitude reservoir is directly applied to the position operator equivalent to a random shift on the momentum displacement of the ion. The numerics shows that the broadening due to the random shift on the momentum is more detrimental to the QW, as reflected by the AFD.

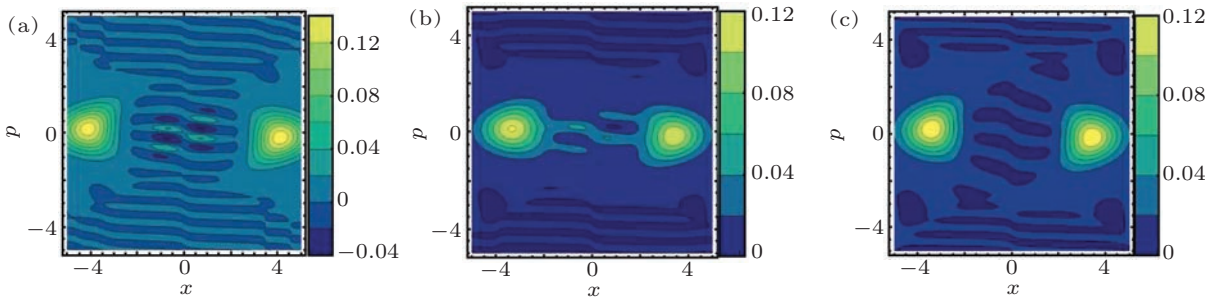


Fig. 3. (colour online) Contour plot of the Wigner function at the tenth step of the QW, (a) without perturbation; (b) under phase damping channel with parameter $q = 0.14$, and (c) under high temperature amplitude reservoir with $q' = 0.18$.

Our scheme provides an experimentally available way to monitor the detrimental influence on the QW by different decoherence sources. In contrast, no previous work for the QW has considered the direct observation of the irreversibility due to decoherence. Some previous work involving imperfection regarding the coin, such as random rotations on the coin[24] and imperfect Hadamard operator,[35] are similar to the phase damping channel considered here. Some other models of imperfection on the walker's position, e.g., imperfect shift in a single optically trapped atoms[36] and dephasing on individual photons in space,[12] are actually close to our study with high temperature amplitude reservoir. Moreover, the high temperature amplitude reservoir broadening the fringes of Wigner function is in fact a heating effect on the motional degrees of freedom of the ion. This broadening has also been considered in Ref. [23] involving the higher-order terms of Lamb–Dicke parameter for achieving more steps in a QW.

3.3. Experimental feasibility

The state-dependent force we employed to produce the state-dependent perturbation on QW has been widely used previously in ion trap systems, e.g. in the implementation of the geometric phase gate[37] and the simulation of a quantum spin system.[38−40] The radial motional modes have also been employed to experimentally simulate frustrated Ising spins.[40] As for our scheme, the accomplishment of the phase damping channel case is very similar to the geometric phase gating in Ref. [37], but with the axial motional mode replaced by the radial motional mode in our case. The case of the high temperature amplitude reservoir resembles the implementation by state-dependent optical dipole force in Ref. [9]. Moreover, we also need to individually address the ions and to carry out some single-qubit operations compensating the time-averaged Stark shift, which are achievable with currently available techniques.

We give a brief estimate below for a realistic implementation of our scheme. It takes about 2.5 μs for accomplishing a phase damping channel case with $\gamma = 2\pi \times 0.4$ MHz with respect to $\omega_r = 2\pi \times 4.334$ MHz,[40] and costs about 2.9 μs for executing a high temperature amplitude reservoir case with $\zeta_m^p = \pi$, $\Omega \approx 2\pi \times 500$ kHz, and $\eta = 0.35$.[9] This implies that we can repeatedly insert the two kinds of the perturbations into the QW system by thousands of times within the decoherence time (e.g., 100 ms in Ref. [40]) of the motional mode.

In our treatment mentioned above, however, we have neglected the effects regarding the higher-order Lamb–Dicke parameters, which might spoil the ideal QW behavior, like the decoherence effects described in this work. To avoid the influence from the higher-order Lamb–Dicke terms on our scheme, we make a simple assessment below. Considering the QW implementation by a trapped ion,[10,23] the detrimental influence is dominantly from the third-order Lamb–Dicke terms in resonance case. Using the result in Ref. [23], we have the contribution of the third-order Lamb–Dicke terms in resonance case scaling as $\eta^2 N^3 \alpha^4/24$ with η the Lamb–Dicke parameter, $\alpha/\sqrt{2}$ the step size of the QW, and N the steps. So if the pulses for inducing decoherence are strong enough compared to those for producing QW, i.e.,

$$\eta^2 N^3 \alpha^4/24 \ll \begin{cases} q\pi, \\ q'\pi \end{cases} \tag{18}$$

for the phase damping channel and high temperature amplitude reservoir respectively, the influence from

the higher-order Lamb–Dicke terms would be negligible in our scheme. Table 1 presents some available values of the parameters meeting Eq. (18), ensuring our scheme to work well in realistic experiments.

Table 1. Assessment of validity of our scheme by considering the third-order Lamb–Dicke parameter in the resonance case, where the parameters are chosen for walking steps $N = 12$ with the left-hand side of Eq. (18) being smaller than the right-hand side by one tenth.

q	α	η	q'	α	η
0.02	0.5	0.037	0.01	0.5	0.026
	$\sqrt{2}$	0.005		$\sqrt{2}$	0.003
0.14	0.5	0.099	0.18	0.5	0.112
	$\sqrt{2}$	0.012		$\sqrt{2}$	0.014

4. Conclusion

In summary, we have proposed an experimentally available scheme for simulating the QW by trapped ions under controllable decoherence. The implementation of the scheme makes it possible to monitor the transition from the QW to random walk by measuring the internal level population of the ions. We have demonstrated that the conditional position shift is more sensitive to the decoherence than the coin toss, which helps us better understand the QW simulation in a realistic environment.

Furthermore, we have employed both the AFD and the position variance to characterize the irreversibility. Despite no strict proof, our calculation has demonstrated that the AFD might be better for this job than the position variance. Finally our idea of experimentally measuring the AFD under controllable decoherence on the QW can also be applied to optically trapped atoms. The decoherence can be controllably introduced by the controlled-phase gate induced by Rydberg blockade[42−44] and the AFD is measured by similar physics to the trapped-ion system we modeled here.

References

[1] Aleliunas R, Karp R, Lipton R, Lovasz L and Rackoff C 1979 *Proceedings of the 20th Annual Symposium on Foundations of Computer Science* p. 218

[2] Selman B, Kautz H A and Cohen B 1996 *DIMACS Series in Discrete Mathematics and Theoretical Computer Science* **26** 1

[3] Childs A M, Farhi E and Gutmann S 2002 *Quantum Infor. Process.* **1** 35

[4] Childs A M and Goldstone J 2004 *Phys. Rev.* A **70** 022314

[5] Shenvi N, Kempe J and Whaley K B 2003 *Phys. Rev.* A **67** 052307

[6] Somma R D, Boixo B, Barnum H and Knill E 2008 *Phys. Rev. Lett.* **101** 130504

[7] Childs A M 2009 *Phys. Rev. Lett.* **102** 180501

[8] Karski M, Förster L, Choi J M, Steffen A, Alt W, Meschede D and Widera A 2009 *Science* **325** 174

[9] Schmitz H, Matjeschk R, Schneider C, Glueckert J, Enderlein M, Huber T and Schaetz T 2009 *Phys. Rev. Lett.* **103** 090504

[10] Zähringer F, Kirchmair G, Gerritsma R, Solano E, Blatt R and Roos C F 2010 *Phys. Rev. Lett.* **104** 100503

[11] Schreiber A, Cassemiro K N, Potoček V, Gabris A, Mosley P J, Andersson E, Jex I and Silberhorn C 2010 *Phys. Rev. Lett.* **104** 050502

[12] Broome M A, Fedrizzi A, Lanyon B P, Kassal I, Aspuru-Guzik A and White A G 2010 *Phys. Rev. Lett.* **104** 153602

[13] Richter P C 2007 *New J. Phys.* **9** 72

[14] Richter P C 2007 *Phys. Rev.* A **76** 042306

[15] Rebentrost P, Mohseni M, Kassal I, Lloyd S and Aspuru-Guzik A 2009 *New J. Phys.* **11** 033003

[16] Lin F and Bao J D 2011 *Chin. Phys.* B **20** 040502

[17] Dur W, Raussendorf R, Kendon V M and Briegel H J 2002 *Phys. Rev.* A **66** 052319

[18] Kendon V and Tregenna B 2003 *Phys. Rev.* A **68** 052305

[19] Romanelli A, Siri R, Abal G, Auyuanet A and Donangelo R 2004 *Physica* A **347** 137

[20] Zhang K 2008 *Phys. Rev.* A **77** 062302

[21] Brun T A, Carteret H A and Ambainis A 2003 *Phys. Rev.* A **67** 032304

[22] Brun T A, Carteret H A and Ambainis A 2003 *Phys. Rev. Lett.* **91** 130602

[23] Xue P, Sanders B C and Leibfried D 2009 *Phys. Rev. Lett.* **103** 183602

[24] López C C and Paz J P 2003 *Phys. Rev.* A **68** 052305

[25] Romanelli A 2009 *Phys. Rev.* A **80** 022102

[26] Annabestani M, Akhtarshenas S J and Abolhassani M R 2010 *arXiv*: 1004.4352v1

[27] Cucchietti F M, Dalvit D A R, Paz J P and Zurek W H 2003 *Phys. Rev. Lett.* **91** 210403

[28] Nielsen M A and Chuang I L 2000 *Quantum Computation and Quantum Information* (Cambridge: Cambridge University Press)

[29] Lee P J, Brickman K A, Deslauriers L, Haljan P C, Duan L M and Monroe C 2005 *J. Opt.* B: *Quantum Semiclass. Opt.* **7** S371

[30] Zhu S L and Wang Z D 2003 *Phys. Rev. Lett.* **91** 187902

[31] Zhu S L, Monroe C and Duan L M 2006 *Phys. Rev. Lett.* **97** 050505

[32] Myatt C J, King B E, Turchette Q A, Sackett C A, Kielpinski D, Itano W M, Monroe C and Wineland D J 2000 *Nature* **403** 269

[33] Turchette Q A, Myatt C J, King B E, Sackett C A, Kielpinski D, Itano W M, Monroe C and Wineland D J 2000 *Phys. Rev.* A **62** 053807

[34] Walls D F and Milburn G J 1994 *Quantum Optics* (Berlin/Heidelberg: Springer-Verlag) p. 63

[35] Mackay T D, Bartlett S, Stephenson L and Sanders B 2002 *J. Phys.* A: *Math. Gen.* **35** 2745

[36] Dür W, Raussendorf R, Kendon V M and Briegel H J 2002 *Phys. Rev.* A **66** 052319

[37] Leibfried D, DeMarco B, Meyer V, Lucas D, Barrett M, Britton J, Itano W M, Jelenkovic B, Langer C, Rosenband T and Wineland D J 2003 *Nature* **422** 412

[38] Porras D and Cirac J I 2004 *Phys. Rev. Lett.* **92** 207901

[39] Friedenauer A, Schmitz H, Glueckert J T, Porras D and Schaetz T 2008 *Nat. Phys.* **4** 757

[40] Kim K, Chang M S, Korenblit S, Islam R, Edwards E E, Freericks J K, Lin G D, Duan L M and Monroe C 2010 *Nature* **465** 590

[41] Schmidt-Kaler F, Gulde S, Riebe M, Deuschle T, Kreuter A, Lancaster G, Becher C, Eschner J, Haffner H and Blatt R 2003 *J. Phys.* B **36** 623

[42] Jaksch D, Cirac J I, Zoller P, Rolston S L, Côté R and Lukin M D 2000 *Phys. Rev. Lett.* **85** 2208

[43] Cubel T, Teo B K, Malinovsky V S, Guest J R, Reinhard A, Knuffman B, Berman P R and Raithel G 2005 *Phys. Rev.* A **72** 023405

[44] Beals T R, Vala J and Whaley K B 2008 *Phys. Rev.* A **77** 052309